DOI: 10.1002/ejic.200600507

Co^{III} Complexes with Square-Planar N_2S_2- and $N_2(SO_2)_2$-Type Ligands as An Active Site Structural Model for Nitrile Hydratase – Biological Implications of an Amidate Coordination

Takuma Yano,[a] Hidekazu Arii,[a] Syuhei Yamaguchi,[a] Yasuhiro Funahashi,[a] Koichiro Jitsukawa,[a] Tomohiro Ozawa,*[a] and Hideki Masuda*[a]

Keywords: Nitrile hydratase / Cobalt / Amidate ligand / Electrophilic interactions / Lewis acids

In an attempt to understand the unique active site structure of nitrile hydratase, four Co^{III} complexes with square-planar N_2S_2- or $N_2(SO_2)_2$-type donor sets, Na[Co^{III}(**L:N_2S_2**)] (**1**-Na), PPh_4[Co^{III}(**L:N_2S_2**)] (**1**-PPh_4), PPh_4[Co^{III}(**L:N_2S_2**)(*t*BuNC)$_2$] (**2**), and PPh_4[Co^{III}{**L:$N_2(SO_2)_2$**}(*t*BuNC)$_2$] (**3**) were synthesized and characterized on the basis of electronic absorption spectroscopy, IR spectroscopy, cyclic voltammetry, and X-ray structural analysis. Both of the crystal structures of complexes **1**-Na and **1**-PPh_4 revealed a square planar structure with N_2S_2 donating atoms, and **2** exhibited an octahedral structure coordinated with two *tert*-butylisocyanide (*t*BuNC) molecules at the axial sites of complex **1**-PPh_4. Complex **3**, which showed an octahedral structure with sulfinate sulfur atoms equatorially coordinated to the center, was synthesized by the treatment of **2** with a suitable oxidant. The reduction potential values from Co^{III} to Co^{II} for complex **3** in solution demonstrated a larger positive shift when compared with those of complexes **1**-PPh_4 and **2**, which indicates that the oxygenation of the sulfur atoms increased the Lewis acidity of the Co^{III} center. Interestingly, the coordination equilibrium, the C=O stretching frequency, and the redox potential for **1**-PPh_4 were all closely related to the acceptor number (AN) of the solvents. Furthermore, the coordination of monodentate *t*BuNC to the axial position of **1**-PPh_4 was dependent on the solvents used. These findings indicate that an electrophilic interaction between the carbonyl oxygen atoms and the solvent molecules control the Lewis acidity of the metal ion. On the other hand, such a solvent dependence was not detected in the S=O stretching frequency of sulfinates **3**. We have concluded that the increase in the redox potential/Lewis acidity of the metal center is a result of the oxygenation of sulfur, and that this increase is controlled by the interaction of the amidate carbonyl oxygen with the secondary coordination sphere. As demonstrated in previous mutation studies, this study suggests that the interaction of the nitrile hydratase active site with the functional groups from the peptide backbone is essential for the catalytic activity of the complex.

Introduction

Nitrile Hydratase (NHase) is an enzyme that hydrates a nitrile compound to the corresponding amide. Because of its high conversion ability, this enzyme has been employed for the industrial production of acrylamide from acrylonitrile under mild conditions.[1] The NHases are largely classified into Fe^{III}-type and Co^{III}-type families.[2–4] *Rhodococcus rhodochrous* J1, which is a bacterium with the typical Co^{III}-type NHase, has been used to produce several kilotons of acrylamide per year.[3–5] The common amino acid sequence (C–**X**–**Y**–C–S–C) of the peptide in the Fe^{III}-type and the Co^{III}-type NHase has been proposed as the metal binding ligand on the basis of the similarity between the EXAFS and its pre-edge spectra[6,7] in addition to homology in significant amino acid sequences.[8]

Recent X-ray structure analysis of both NHase types revealed that the metal centers are surrounded by two amide nitrogen atoms and two cysteine sulfur atoms in the equatorial plane with a cysteine sulfur and an oxygen atom (H_2O or OH^-), or a cysteine sulfur and a NO group, at the axial sites for the Co^{III}- or Fe^{III}-types, respectively.[9–12] Interestingly, two equatorially coordinated cysteine sulfur atoms are oxygenated to a sulfenate and a sulfinate, respectively, and the two nitrogen atoms contribute as an amidate ligand. Such a unique structure is very interesting in relation to its hydration mechanism in biological systems.

In such a hydration enzyme, a higher Lewis acidity of the metal center should be required, although M–OH^- (or M–OH_2) or M–NCR are proposed as possible active intermediates. On the basis of the HSAB rule, the N^- and S^- ions employed in the enzymes may stabilize the higher oxidation state of the metal center, and the attached electron-withdrawing carbonyl group along with the sulfenyl and sulfinyl

[a] Graduate School of Engineering, Nagoya Institute of Technology,
Gokiso-cho, Showa-ku, Nagoya 466–8555, Japan
Fax: +81-52-735-5228
E-mail: masuda.hideki@nitech.ac.jp

Supporting information for this article is available on the WWW under http://www.eurjic.org or from the author.

oxygen atoms may reduce the electron density on the metal center to induce a higher acidity. It is quite apparent that both functional groups are very important for the enzymatic reaction. However, the use of the mutant Fe-type NHases that did not contain oxygenated sulfur atoms did not show any hydration reaction, which indicates that the oxygenated sulfur atoms are essential for the enzymatic activity.[13]Most studies that use model complexes have focused on the effect of the oxidation of sulfur. For example, several Co^{III} and Fe^{III} complexes with pentadentate ligands that contain an imine,[14] an amide,[15,16] or an amine[17] group and sulfur atoms have been synthesized and studied. Among them, Mascharak and coworkers[15a] have prepared the complex [Co(PyPS)(CN)] with the use of the amide-type ligand, which was easily replaced by a H_2O molecule. The coordinated water molecule catalytically hydrated acetonitrile to acetamide at pH = 9.5. The addition of an oxidant to the solutions of the complexes afforded the corresponding sulfur-oxidized species.[15b] For the Co^{III} mononuclear complex, the Co^{III} species with a sulfinate was isolated. Hydration of acrylonitrile with this sulfonate–Co^{III} complex proceeded three times faster than that of the complex with two unoxidized sulfur atoms even in acidic media (pH = 8.0). They concluded that the oxygenation of sulfur would make the acidity of the coordinated H_2O molecule increase. Other groups have prepared and characterized the Co^{III} and Fe^{III} complexes with tetradentate planar ligands that contain two amide nitrogen atoms and two thiolate sulfur atoms in the same coordination environment as the NHase active sites,[18,19] and they also succeeded in the generation of sulfinate and sulfenate species by the oxidation of the coordinated sulfur atoms.[18a,18b,19a,19b] However, all of them showed octahedral structures with two monodentate ligands at the axial positions.[18a,18b,19a,19b] Recently, Artaud and coworkers reported that in the synthesis of the $N_2(SO_2)_2$-type Co^{III} complex with a CN^- ion at the apical position, the octahedral complex with a hydroxo ion at another axial position was derived.[20] Thus, the oxygenation of sulfur in the equatorial plane has been described to be one of the important factors that leads to an octahedral geometry.

Few have paid attention to the amidate group. However, a mutation study of Fe-containing NHase demonstrated that βR56K, whose Arg56 residue is replaced by lysine and coordinated to the sulfinate and sulfenate oxygen atoms through a hydrogen bond, demonstrated only ca. 1% of the reactivity of the native species.[21] For the βY68F mutant of the Co^{III}-type NHase, the enzymatic activity drastically decreased, although it was positioned at a distance from the active site.[22] Moreover, the OH group of tyrosine in βTyr68 is linked to the carbonyl oxygen of the active site through water molecules and the hydrogen bond network around βArg56. βArg56 is, itself, also connected to βTyr68. These facts indicate that the hydrogen-bonding interactions of the coordinating functional groups with the outer sphere strongly contribute to the appearance of the NHase activity. Therefore, we focused on the biological role of the amidate carbonyl group and synthesized two Co^{III} complexes with N_2S_2-type ligands, *N*,*N*′-bis(2-mercapto-2-methylpropionyl)-1,3-diaminopropane (H_4**L**) and the corresponding sulfinic acid derivative [**L**:$N_2(SO_2)_2$; the two sulfur atoms of H_4**L** are oxygenated to sulfinates]. In order to evaluate the influence of the outer sphere, the coordination behaviors of the axial sites of the Co^{III} complex with *tert*-butylisocyanide (*t*BuNC) were evaluated. Isocyanides such as isobutylisocyanide[23] and cyclohexylisocyanide[24] are often employed because of their well-known ability to act as coordinative monodentate ligands for NHase.

Results and Discussion

Crystal Structures of Na[Co(L:N_2S_2)]3H_2O (1-Na), PPh_4[Co^{III}(L:N_2S_2)]H_2O (1-PPh_4), PPh_4[Co^{III}(L:N_2S_2)$_2$-(*t*BuNC)$_2$] (2), and PPh_4[Co^{III}{L:$N_2(SO_2)_2$}(*t*BuNC)$_2$]-EtOH (3)

The N_2S_2-type ligand, H_4**L**, which provides electron-donating atoms similar to the equatorial coordination environment of the NHase active center, was used for the construction of the model complexes. The Co^{III} complex with **L**, Na[Co(**L**:N_2S_2)] (**1**-Na), was prepared by the air-oxidation of the corresponding Co^{II} complex derived from the reaction of $CoCl_2$ and H_4**L** in DMF. Recrystallization of the compound from an acetonitrile/diethyl ether solution afforded a single crystal suitable for X-ray analysis, whose

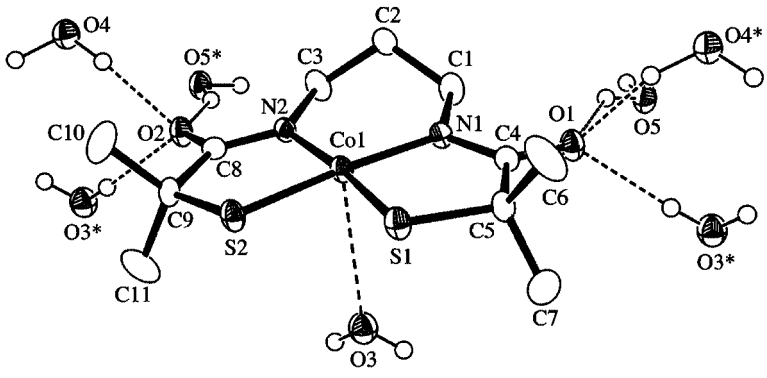

Figure 1. An ORTEP view of Na[Co(**L**:N_2S_2)] (**1**-Na) with solvated water molecules, which shows 50% probability ellipsoids. H atoms are omitted for clarity except for those of the water molecules.

crystal data and molecular structure are shown in Table 2 and Figure 1, respectively. Two $[Co^{III}(\mathbf{L}:N_2S_2)]^-$ and two Na^+ ions are included together with six water molecules in a unit cell (Figure S1). Selected bond lengths and angles are listed in Table 1. Complex **1**-Na has a square-planar geometry with N_2S_2 donor atoms as well as the equatorial coordination in the active site of NHase.[9–12] The bond lengths around the metal center [Co1–N1 = 1.919(3), Co1–N2 = 1.918(3), Co1–S1 = 2.141(1), Co1–S2 = 2.142(1) Å] are comparable to those of the Co^{III} complexes with amide (Co–N = 1.86–1.90 Å) and thiolate coordinations (Co–S = 2.13–2.14 Å) that were previously reported.[18c,19c] Each carbonyl oxygen of the ligand **L** was significantly coordinated to three water molecules [$O_{carbonyl}\cdots O_{water}$ = 2.84–2.91 Å] in the crystal. Furthermore, one water molecule also weakly approaches the Co^{III} ion with a bond length of 3.20 Å at the axial position, which is very similar to the case of Co-type NHase.[11]

One more Co^{III} complex with **L**, $PPh_4[Co(\mathbf{L}:N_2S_2)]$ (**1**-PPh_4), was also prepared by the ion-exchange of **1**-Na in an aqueous solution of PPh_4Cl. Complex **1**-PPh_4 was obtained as a single crystal suitable for X-ray analysis, whose crystal data and molecular structure are shown in Table 2 and Figure 2, respectively. Four $[Co^{III}(\mathbf{L}:N_2S_2)]^-$ anions and four PPh_4^+ cations are included together with four water molecules in a unit cell (Figure S2). Selected bond lengths and angles are listed in Table 1. The molecular structure of complex **1**-PPh_4 was essentially the same as that of **1**-Na. The bond lengths around the metal center [Co1–N1 = 1.902(3), Co1–N2 = 1.896(3), Co1–S1 = 2.138(1), Co1–S2 = 2.144(1) Å] are in the range of those of the Co^{III} complexes with amide (Co–N = 1.86–1.90 Å) and thiolate coordinations (Co–S = 2.13–2.14 Å) that were previously reported.[18c,19c] However, a detailed comparison of those of **1**-Na and **1**-PPh_4 indicated that the Co–N bonds of **1**-PPh_4 were significantly different from those of **1**-Na, although the Co–S bonds was almost the same as those of **1**-Na. This behavior is apparently influenced by the number of hydrogen bonds between water molecules and the amidate carbonyl oxygen atoms. The two carbonyl oxygen atoms of **1**-PPh_4 are hydrogen-bonded with one water molecule each. However, each carbonyl oxygen of **1**-Na is coordinated to three water molecules of a water–sodium cluster. The C=O [1.250(4), 1.243(4)], C_{amide}–N [1.341(4), 1.348(4)], and Co–N [1.902(3), 1.896(3)] bond lengths of **1**-PPh_4 with one water molecule for one carbonyl oxygen demonstrated significant alternations of shorter, longer, and shorter lengths in comparison with those of **1**-Na, C=O [1.263(4), 1,257(4)], C_{amide}–N [1.330(4), 1.332(3)], and Co–N [1.919(3), 1.918(3)], with three hydrogen bonds for each carbonyl oxygen. This alternation in bond lengths provides evidence for the fact that the amidate carbonyl oxygen is affected by the interaction of the secondary sphere.

An octahedral Co^{III} complex, $PPh_4[Co^{III}(\mathbf{L}:N_2S_2)(t\text{BuNC})_2]$ (**2**), where two of the axial positions of **1** are occupied by *tert*-butylisocyanide (*t*BuNC) molecules, was also isolated from an ethanol solution that contained a large amount of *t*BuNC as a red-colored single-crystal suitable for X-ray analysis. Crystal data is listed in Table 2 and the ORTEP view of the anion moiety of **2** is shown in Figure 3. Four $[Co^{III}(\mathbf{L}:N_2S_2)(t\text{BuNC})_2]^-$ anions and four

Table 1. Selected bond lengths [Å] and angles [°] for Na[Co($\mathbf{L}:N_2S_2$)](**1**-Na) and $PPh_4[Co(\mathbf{L}:N_2S_2)]$(**1**-$PPh_4$) and PPh_4-$[Co(\mathbf{L}:N_2S_2)(t\text{BuNC})_2]$(**2**) and $PPh_4[Co\{\mathbf{L}:N_2(SO_2)_2\}(t\text{BuNC})_2]$-(**3**).[a]

	1-Na		
	Bond lengths [Å]		
Co1–N1	1.919(3)	O1···O3	2.86
Co1–N2	1.918(3)	O1···O4	2.91
Co1–S1	2.141(1)	O1···O5	2.84
Co1–S2	2.142(1)	O2···O3	2.86
O1–C4	1.263(4)	O2···O4	2.91
O2–C8	1.257(4)	O2···O5	2.84
N1–C4	1.330(4)		
N2–C8	1.332(3)		
	Bond angles [°]		
N1–Co1–N2	98.0(1)	S1–Co1–N2	173.99(9)
S1–Co1–S2	86.12(4)	S2–Co1–N1	173.96(9)
S1–Co1–N1	87.89(9)	S2–Co1–N2	87.92(9)
	1-PPh_4		
	Bond lengths [Å]		
Co1–N1	1.902(3)	N1–C4	1.341(4)
Co1–N2	1.896(3)	N2–C8	1.348(4)
Co1–S1	2.138(1)	O1···O3	2.83
Co1–S2	2.144(1)	O2···O3	2.82
O1–C4	1.250(4)		
O2–C8	1.243(4)		
	Bond angles [°]		
N1–Co1–N2	97.4(1)	S1–Co1–N2	174.07(9)
S1–Co1–S2	86.51(4)	S2–Co1–N1	171.07(9)
S1–Co1–N1	87.95(9)	S2–Co1–N2	88.50(9)
	2		
	Bond lengths [Å]		
Co1–N1	1.973(2)	O1–C3	1.258(3)
Co1–S1	2.2491(8)	N1–C3	1.318(3)
Co1–C7	1.844(3)	N2–C7	1.150(4)
	Bond angles [°]		
N1–Co1–N1*	99.7(1)	S1–Co1–N1*	174.69(6)
S1–Co1–S1*	89.12(4)	C7–Co1–C7*	179.8(2)
S1–Co1–N1	85.57(6)	Co1–C7–N2	176.8(3)
	3		
	Bond lengths [Å]		
Co1–N1	1.996(2)	O1–C4	1.249(4)
Co1–N2	1.986(2)	O4–C8	1.252(3)
Co1–S1	2.1830(7)	N1–C4	1.320(3)
Co1–S2	2.1723(7)	N2–C8	1.322(3)
Co1–C12	1.874(3)	N2–C7	1.148(4)
Co1–C17	1.847(3)	N4–C17	1.148(3)
		O1···O7	2.66
	Bond angles [°]		
N1–Co1–N2	97.64(8)	S2–Co1–N1	176.85(6)
S1–Co1–S2	93.07(3)	S2–Co1–N2	83.97(6)
S1–Co1–N1	85.25(6)	C12–Co1–C17	175.6(1)
S1–Co1–N2	176.70(6)	Co1–C12–N3	174.8(2)
		Co1–C17–N4	174.4(2)

[a] The atoms with and without * are related by a crystallographic mirror plane between each other.

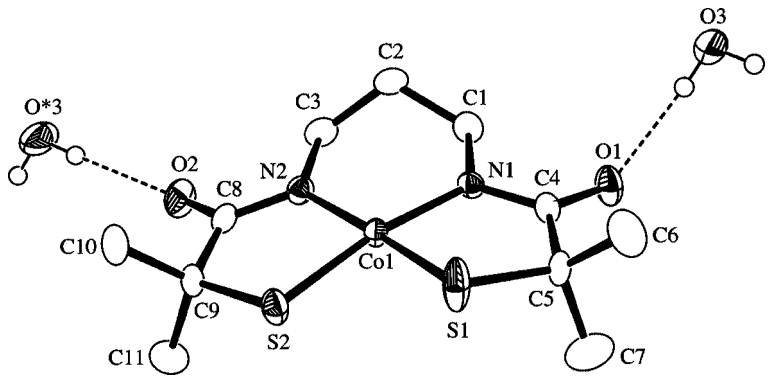

Figure 2. An ORTEP view of $[Co(\mathbf{L{:}N_2S_2})]^-$ anion part of complex **1** with solvated water molecules, which shows 50% probability ellipsoids. H atoms are omitted for clarity except for those of the water molecules.

PPh_4^+ cations are included in a unit cell. Selected bond lengths and angles are listed in Table 1. The *tert*-butyl group of the axial ligands and the propylene group of the equatorial ligand are disordered. The octahedral coordination formed by the axial binding of *t*BuNC ligands to **1** induces longer $Co–N_{amide}$ and Co–S bonds in comparison with those of **1**, although the average bond lengths of Co–S [2.2491(8) Å] and $Co–N_{amide}$ [1.973(2) Å] are within the range of those of the previously reported octahedral Co^{III} complexes with thiols and/or amides (Co–S = 2.22–2.27 Å, Co–N = 1.91–2.00 Å).[18a,19a,19b,19d] The detailed examination of the bond lengths around the Co center indicate that the Co–N and Co–S bonds are clearly elongated in comparison with those of complexes **1**-PPh_4 and **1**-Na, which is explained by the coordination of the *t*BuNC molecules.

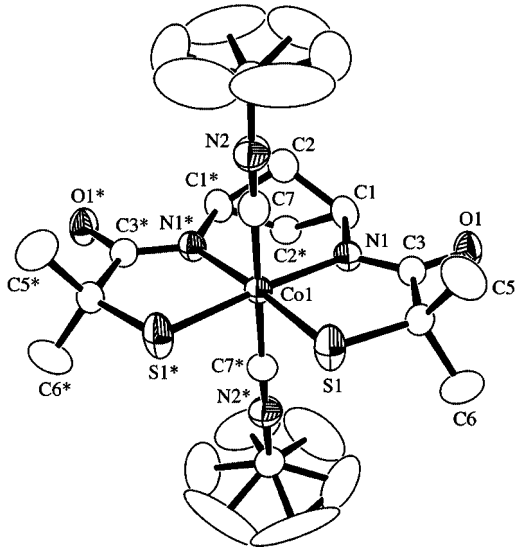

Figure 3. An ORTEP view of $[Co(\mathbf{L{:}N_2S_2})(t\text{BuNC})_2]^-$ anion part of complex **2**, which shows 50% probability ellipsoids.

Furthermore, treatment of complex **2** with 30% H_2O_2 according to a previously-reported procedure[19b] with some modifications successfully afforded the corresponding complex, $PPh_4[Co\{\mathbf{L{:}N_2(SO_2)_2}\}(t\text{BuNC})_2]$ (**3**), of which the two thiolate groups were oxygenated to sulfinates. The crystal data of a single crystal obtained from an EtOH/ether solution is listed in Table 2, and the molecular structure revealed the formation of complex **3**, as depicted in Figure 4. Selected bond lengths and angles are listed in Table 1. The bond lengths around the metal center [Co1–N1 = 1.996(2), Co1–N2 = 1.986(3), Co1–S1 = 2.1830(7), Co1–S2 = 2.1723(7) Å] lay within the range of those of the previously reported Co^{III} complexes with amide and sulfinate groups (Co–N = 1.94–2.00 Å, Co–S = 2.21–2.23 Å).[18a,19b] The Co–N and Co–S bond lengths of **3** are longer than those of **1**-PPh_4 and **1**-Na, which is reasonably explained by the coordination of the *t*BuNC molecules. The oxygenation of sulfur in complexes **2** and **3** induced the lengthening of the Co–N bonds and the shortening of the Co–S bonds, although it did not influence the Co–C(*t*BuNC) bond lengths. The carbonyl oxygen atoms of the ligand $\mathbf{L{:}N_2(SO_2)_2}$ were also significantly coordinated to an ethanol molecule. Such a hydrogen bond was not found around the sulfinate oxygen atoms.

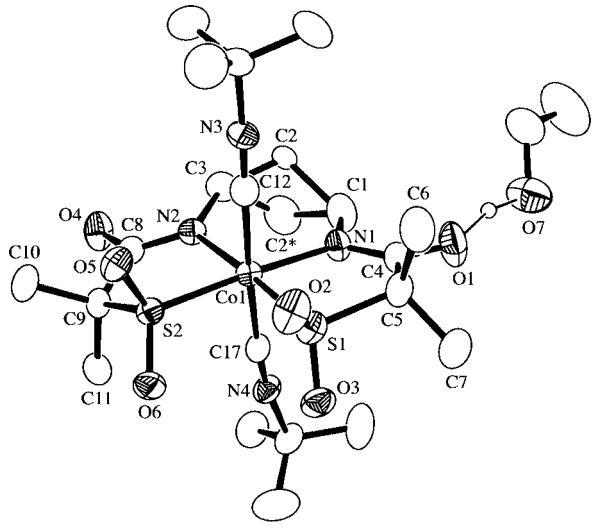

Figure 4. An ORTEP view of $[Co\{\mathbf{L{:}N_2(SO_2)_2}\}(t\text{BuNC})_2]^-$ anion part of complex **3**, which shows 50% probability ellipsoids. H atoms are omitted for clarity.

Coordination Equilibrium of *t*BuNC to 1 in Solution

The electronic absorption spectrum of complex **1** showed a ligand-to-metal charge transfer (LMCT) band around 600 nm (ε = 3800 $M^{-1}cm^{-1}$), which is characteristic of a square planar Co^{III} complex with sulfur atoms.[18c,19c] The coordination behavior of the monodentate ligands at the axial positions of **1** was studied with anionic ligands, such as sodium phenolate, sodium thiophenolate, tetraethylammonium thiocyanate (Et_4NSCN), and tetraphenylphosphonium cyanide (PPh_4CN), and with neutral ligands, such as water, 4-phenylpyridine, and *tert*-butylisocyanide (*t*BuNC). Significant spectral changes were observed only when PPh_4CN or *t*BuNC was added to a solution of **1** at ambient temperature. For PPh_4CN and *t*BuNC, the absorption spectra had a change in the isosbestic point at 301 nm and 317 nm in EtOH, respectively (Figure S3). It is clear that both the monodentate ligands coordinate at the axial sites of **1**. In the case of *t*BuNC, such a spectral change in the isosbestic point of the LMCT band was also observed in other solvents, which indicates that the Co^{III} complex reacted with *t*BuNC to form octahedral complex **2**.[18a,19c] Formation of the octahedral complex was also supported by the fact that the finally obtained spectrum was in good agreement with that of **2**. The axial coordination of *t*BuNC in complex **2** is also clear from the fact that complexes **1** and **2** show a paramagnetism and a diamagnetism, respectively, in their ^1H NMR spectra (Figure S4). It should be noted that the octahedral coordination of **2** was maintained without any release of the axial ligands in an aqueous solution, although the coordination of the ligands was not conserved in organic solvents (Figure S5). Therefore, we can conclude that the octahedral structure of complex **2** is maintained in water, which is comparable to the effect of the oxygenation of the sulfur atoms.

For the complete formation of octahedral species in acetone, the addition of a 1000-fold excess of *t*BuNC in methanol was required. The electrostatic effect on the metal center that is caused by the interaction between the coordinated amide groups and the solvent is best understood through the examination of the equilibrium experiment with complex **1** for the following reasons: (1) the sulfur atoms of the tetradentate ligand are not easily air-oxidized in the preparation of complex **1**; therefore, direct interactions of the oxygenated sulfinate oxygen atoms with the solvent molecules of the secondary coordination sphere can be eliminated, (2) the solvation of the neutral monodentate ligand *t*BuNC that is coordinated to the complex can be excluded, (3) the axial coordination of the ligands to the square-planar complex induces a higher lability of the complex. Therefore, we investigated the effect of solvents on the equilibrium constant (K_s) [Equation (1)].

$$[Co^{III}(\mathbf{L}{:}\mathbf{N_2S_2})]^- + 2\ t\text{BuNC} \overset{K}{\rightleftharpoons} [Co^{III}(\mathbf{L}{:}\mathbf{N_2S_2})(t\text{BuNC})_2]^- \quad (1)$$

With the use of the intensity change in the LMCT band (700 nm), the equilibrium constants for the reaction have been estimated. Equation (2) was derived on the basis of Equation (1) with material balances taken into account.

$$\log\{(A_0-A)/A\} = 2\log[C_{Bu}-\{2(A_0-A)/A_0\}C_{CoL}] + \log K_s \quad (2)$$

Here, A_0 and A represent the absorption intensities of the $[Co^{III}(\mathbf{L}{:}\mathbf{N_2S_2})]^-$ solution and that of the mixed solution of $[Co^{III}(\mathbf{L}{:}\mathbf{N_2S_2})]^-$ and $[Co^{III}(\mathbf{L}{:}\mathbf{N_2S_2})(t\text{BuNC})_2]^-$, respectively. C_{Bu} and C_{CoL} are the total concentrations of *t*BuNC and the $[Co^{III}(\mathbf{L}{:}\mathbf{N_2S_2})]^-$ solutions, respectively. The relationship between the absorbance term of the complex versus the concentration term of added *t*BuNC was plotted according to Equation (1) and showed a linear relationship with a slope of 2, within experimental error. This indicates that two *t*BuNC molecules are coordinated to the Co^{III} complex in all of the solvents. This result was also confirmed from the similarity in the absorption spectrum of **2** as described above. The equilibrium constant, K_s, clearly showed the solvent dependence (Table S1); they gradually decreased as follows: H_2O/MeOH (3:7) > H_2O/MeOH (1:9) > methanol > ethanol > 2-PrOH > dichloromethane > acetone. The constant, K_s, demonstrated a linear relationship only for the acceptor number (AN)[25–28] of solvents which is an index of electrophilicity[28,29] [Figure 5 (■)]. K_s did not show this relationship for any other physical parameters such as a donor number[29,30] or a dielectric constant. This result indicates that an interaction of the electrophilic solvent with **1** makes the axial coordination of *t*BuNC easier.

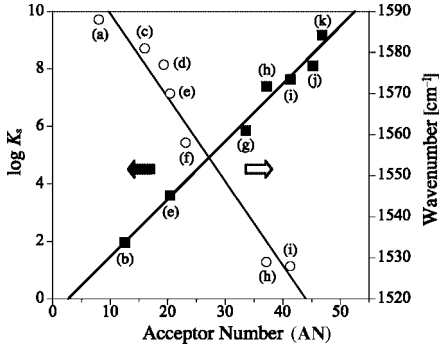

Figure 5. Plots of logK_s values (■) and C=O stretching vibration values (○) for complex **1** versus ANs of organic solvents. (a) THF; (b) acetone; (c) DMF; (d) MeCN; (e) CH_2Cl_2; (f) $CHCl_3$; (g) 2-propanol; (h) EtOH; (i) MeOH; (j) H_2O/MeOH [1:9 (v/v)]; (k) H_2O/MeOH [3:7 (v/v)].

Infrared Spectra of 1 and 3 in Organic Solvents

As described above, the coordination of *t*BuNC at the axial sites of **1** depends on the electrophilic solvents, whose solvent dependence should be considered to be caused by the interaction of complex **1** with the solvent molecules. The electron-rich carbonyl oxygen atoms of the ligand **L** can also interact with the electrophilic solvent. Therefore, IR spectra were obtained for **1** and **3** in order to identify the interaction site of the complexes with the solvent molecules.

The IR spectra of sample solutions without the Co^{III} complex were measured as a base line. A difference spectrum between the solution of **1** and the base line was then adopted. Interestingly, the frequencies assigned to the stretching vibration of C=O are dependent on the solvents within the range of 1520–1590 cm^{-1} as listed in Table S2. The C=O stretching vibrations are linearly dependent on the ANs as shown in Figure 5 (○), which suggests that the axial coordination is predominantly controlled by the interaction of the solvent molecules with the carbonyl oxygen atoms.

The solvent-dependent shift of the C=O stretching frequency was also observed for **3**, and the C=O stretching vibration for **3** (Table S3) showed a similar shift to that of **1**, as shown in Figure 6 (■). However, in the same solvents the absorption bands in **3** appeared in a higher energy region compared with those of **1**. An increase in the C=O bond strength of **3** compared with that of **1** induced a decrease in the Co–N bond strength, which may be explained in terms of the coordination saturation and strong *trans* influence of SO_2.[15c] On the other hand, remarkably, the stretching frequency of the S=O group, which is considered as another possible interaction site for the solvents, did not show any significant shift [Figure 6 (○), Table S4]. The vibration responsible for N≡C in **3** is also linearly dependent on the ANs of the solvents (Figure S6, Table S5). The linear relationship indicates that the interaction of the carbonyl oxygen atoms with the solvent molecules causes a change in the N≡C vibration, while the sulfinate oxygen did not show any interaction with the solvents as described above. The N≡C vibration showed a significantly higher energy shift with an increase in AN, which is similar to the case of the oxidized sulfur atoms.[18a] This result suggests that the attractive interaction of the carbonyl oxygen atoms with the solvent molecules causes an increase in the Lewis acidity of the Co^{III} center.

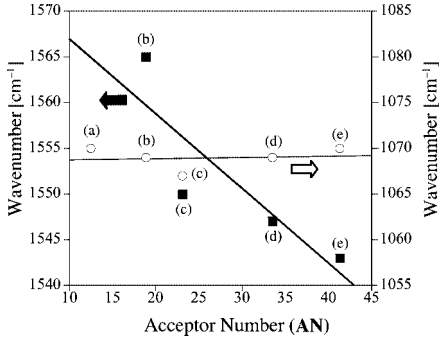

Figure 6. Plots of C=O (■) and S=O stretching vibration values (○) for complex **3** versus ANs of organic solvents. (a) Acetone; (b) MeCN; (c) $CHCl_3$; (d) 2-PrOH; (e) MeOH.

Redox Behaviors of 1, 2 and 3 in Organic Solvents

The solvent dependence of the C=O stretching vibrations that appeared for complexes **1** and **3** must also influence the acidity of the metal center, so the electrochemical properties of the complexes was investigated with the use of cyclic voltammetry with an Ag/Ag^+ reference electrode. The voltammogram of **1** exhibited only one quasi reversible redox wave assignable to Co^{III}/Co^{II} with $\Delta E \approx 100$ mV and $i_p/i_c \approx 1.0$ within the experimental potential range (–1.7 V to –1.1 V). The electrochemical parameters are listed in Table S5, in which the redox potentials have been standardized to the Fc/Fc^+ potential. The redox potential is high enough to maintain the Co center in the 3+ oxidation state and is consistent with those of previously reported N_2S_2-type Co complexes that contain two amidate nitrogen atoms and two sulfur atoms as coordinating atoms.[31–33] The redox potential in methanol is clearly much higher than that in acetone, which is in agreement with the tendencies for the equilibrium constant K_s and the C=O stretching vibrations. The solvent dependence of the results led us to expect that the Lewis acidity of the Co^{III} center could effectively be controlled by the interaction of **1** with the solvent molecules. The redox potential value ($E_{1/2}$) assignable to Co^{III}/Co^{II} of **1**, as expected, exhibited a solvent dependency with a linear relation to the AN values of the solvents; that is, –1.12 V versus Fc/Fc^+ in MeOH (AN = 41.3) and –1.73 V in THF (AN = 8.0), respectively (Figure 7, Table S6). The redox potential values showed a significantly larger positive shift with an increase in AN, which suggests that the attractive interaction of the carbonyl oxygen atoms with the solvent molecules causes an increase in the Lewis acidity of the Co^{III} center and promotes the axial coordination of a monodentate ligand. On the basis of such a linear relation, the ideal redox potential values of **1** in an aqueous solution (AN = 54.8) and in a noninteracting solvent (AN = 0) were estimated to be –0.93 and –1.89 V, respectively, which implies that the interaction of the amidate carbonyl group with the water molecules causes a shift in the redox potential for the Co^{III} complex by ca. 1 V in comparison with that of a noninteracting solvent.

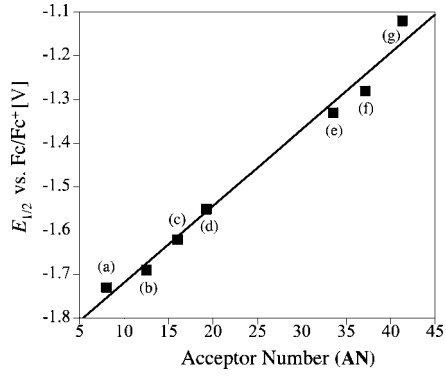

Figure 7. Plots of $E_{1/2}$ for complex **1** versus ANs of organic solvents. (a) THF; (b) acetone; (c) DMF; (d) MeCN; (e) 2-PrOH; (f) EtOH; (g) MeOH.

Furthermore, the reduction potential of complex **3** in MeOH was observed at –1.27 V and that of **2** in the presence of a large amount of *t*BuNC in a MeOH solution was detected at –2.18 V, which indicates that the oxygenation of the sulfur atoms raises the reduction potential of the Co^{III}

complex by ca. 0.9 V. The octahedral structure of complex **2** that is maintained in water is comparable to the effect of the oxygenation of the sulfur atoms. These findings indicate that the attractive interaction between the carbonyl oxygen atoms and the water molecules can control the Lewis acidity of the metal ion as well as the effect of the oxygenation of the sulfur atoms. Consequently, complex **2**, as described above, can maintain the octahedral structure in an aqueous solution (AN = 54.8) without the release of the axial ligands.

Biological Implications

In the crystal structures of both the Co- and Fe-containing NHases,[9–12] the sulfenate and the sulfinate oxygen atoms interact with the arginine residue through hydrogen bonds as described above, and the amidate carbonyl oxygen atoms are coordinated to water molecules. Moreover, the water molecules form a hydrogen bonded network with other water molecules that starts from the tyrosyl oxygen (βTyr68 in Co^{III}-type NHases, Figure 8). It has recently been reported by Miyanaga et al. that the mutant of Co^{III}-type NHase, βY68F, where the hydrogen bonded network is destroyed by the replacement of tyrosine by phenylalanine, does not show significant hydratase function.[22] Miyanaga et al. have explained it on the basis of the crystal structures as follows: βTyr68 contributes to the capture of a substrate or an imidate intermediate through the hydrogen bonds.[22] With the consideration of this report[22] and our results, we can propose that a higher Lewis acidity of the central metal ion is required for the axial coordination of the ligands, which is important for the enzymatic reaction, and may finely be regulated by the hydrogen bonded network from tyrosine to the amidate oxygen atoms through water molecules. From the fact that the S=O group did not show an electrophilic interaction,[28,29] we can conclude that the sulfinate oxygen atoms do not contribute to the control of the Lewis acidity of the central metal. If the Lewis acidity of the central metal can be sensitively controlled by these hydrogen bonding interactions, the reaction will rapidly proceed and the reaction product will also be rapidly released from the central metal ion. In the crystal structures of **1**-PPh_4, **1**-Na, and **3** the carbonyl oxygen atoms of the ligands **L** and **L:$N_2(SO_2)_2$** are coordinated to water and ethanol molecules, respectively. Furthermore, as shown in the crystal structure of complex **1**-Na, three hydrogen bond interactions with three water molecules for each carbonyl oxygen influenced the Co–*N*–C–O bonding system. However, such an interaction was not found in the sulfinyl oxygen atoms of **3**, which may suggest that the sulfinyl oxygen groups do not significantly interact with the solvent molecules.

In conclusion, this paper describes that the hydration reaction in NHase is significantly controlled by the amidate groups as well as the oxygenated sulfur groups.

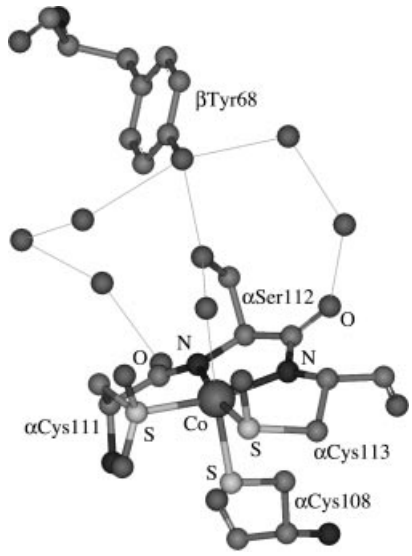

Figure 8. Hydrogen bonding networks near the active site of NHase: hydroxy oxygen of βTyr68 hydrogen-bonded to amide carbonyl oxygen atoms by water molecules.

Experimental Section

Reagents and Technique: All manipulations were performed with Schlenk technique under an Ar atmosphere or in a glove box. Reagents in this study were purchased in reagent grade from Wako Pure Chemical Industries Ltd. or Tokyo Kasei Kogyo Co. Ltd. and used without further purification. Solvents in reagent grade were purchased from Wako Pure Chemical Industries Ltd. and Kanto Kagaku Co. Inc. and distilled twice prior to use.

Synthesis of H_4L: 2-benzylthio-2-methylpropionic acid chloride was synthesized as described previously.[34] The acid chloride (12.77 g, 50.00 mmol) was added dropwise to a THF solution containing 1,3-diaminopropane (1.85 g, 25.00 mmol) and triethylamine (5.06 g, 50.00 mmol). After filtration, a 1 M HCl aqueous solution was added to the filtrate and evaporated. Addition of diethyl ether to the concentrated solution afforded a white powder which was identified as an *S*-benzylated **L** by ^{1}H NMR spectroscopy, whose powder (2.00 g, 4.36 mmol) was dissolved in THF (20 mL) and treated with liquid ammonia at –78 °C. To this solution was added sodium (1.91 g, 82.95 mmol), which was stirred vigorously for 30 min. After the excess ammonia was removed by evaporation at room temperature, the solution was adjusted to pH 3 with 1 M $KHSO_4$. The product was extracted with ethyl acetate and the solvent evaporated. ^{1}H NMR (300 MHz, $CDCl_3$): δ = 1.63 (s, 12 H), 1.70 (m, 2 H), 2.29 (s, 2 H), 3.28 (q, 4 H), 7.83 (s, 2 H) ppm.

Preparation of Na[Co(L:N_2S_2)] (1-Na) and PPh_4[Co(L:N_2S_2)] (1-PPh_4): Na[Co(**L**:N_2S_2)] (**1**-Na) was prepared according to the literature with some modifications.[18,19] Recrystallization of the compound from acetonitrile/diethyl ether afforded a single crystal in atmosphere. Addition of PPh_4Cl (269.4 mg, 0.72 mmol) to an aqueous solution (20 mL) of the sodium salt (256.3 mg, 0.72 mmol) afforded a single crystal of PPh_4[Co(**L**:N_2S_2)] (**1**-PPh_4). $C_{35}H_{40}CoN_2O_3PS_2$ (690.74): calcd. C 60.86, H 5.84, N 4.06; found C 60.93, H 5.77, N 4.03. Electronic absorption spectra ($CHCl_3$): λ_{max} [ε (M^{-1} cm^{-1})] = 312 (7300), 443 (sh), 640 (2600) nm.

Preparation of PPh_4[Co(L:N_2S_2)(*t*BuNC)$_2$] (2): Monodentate ligand, *t*BuNC, (200 μL, 1.76 mmol) was added to an acetonitrile solution (150 μL) containing PPh_4[Co(**L**:N_2S_2)] (3 mg,

$0.43 \cdot 10^{-2}$ mmol). A red crystal was isolated by the slow diffusion of diethyl ether into the solution at 0 °C. $C_{45}H_{56}CoN_4O_2PS_2$ (838.99): calcd. C 64.42, H 6.73, N 6.68; found C 64.14, H 6.60, N 6.47. Selected IR bands (KBr): $\tilde{\nu}$ = 2176 (s, CN), 1535 (s, CO) cm^{-1}. ^1H NMR (300 MHz,D_2O): δ = 1.36 (s, 12 H, CH_3), 1.49 (s, 18 H, *t*Bu), 1.75 (t, 2 H, CH_2), 3.79 (t, 4 H, CH_2), 7.72 (m, 20 H, Ph) ppm. Electronic absorption spectra (H_2O): λ_{max} [ε ($M^{-1}cm^{-1}$)] = 294 (12800), 360 (sh) nm.

Preparation of PPh_4[Co{L:$N_2(SO_2)_2$}(*t*BuNC)$_2$] (3): To an ethanol solution (1 mL) containing PPh_4[Co(**L:N_2S_2**)] (83 mg, 0.12 mmol) was added *t*BuNC (191 μL, 1.44 mmol). After the solution was stirred for 10 min, 30% H_2O_2 (0.62 mL, 5.45 mmol) was added dropwise to the ethanol solution at –10 °C. The solution was left to stand for 3 h at –10 °C. A crude compound was obtained by the addition of diethyl ether into the solution. Recrystallization of the compound from ethanol/diethyl ether afforded a single crystal suitable for X-ray analysis. $C_{47}H_{64}CoN_4O_8PS_2$ (967.07): calcd. C 58.37, H 6.67, N 5.79; found C 58.14, H 6.50, N 6.00. Selected IR bands (KBr) : $\tilde{\nu}$ = 2199 (s, CN), 1552 (s, CO), 1214 and 1071 (s, SO) cm^{-1}. ^1H NMR (300 MHz, [D_6]DMSO): 1.15 (s, 12 H, CH_3), 1.34 (s, 18 H, *t*Bu), 3.16 (t, 6 H, CH_2), 7.83 (m, 20 H, Ph) ppm. Electronic absorption spectrum (EtOH): λ_{max} [ε ($M^{-1}cm^{-1}$)] = 273 (9700), 313 (21400), 400 (sh) nm. ESI-MS ([Co^{III}(**L:$N_2(SO_2)_2$**)(*t*BuNC)$_2$]$^-$): *m*/*z* (%) = 563.

X-ray Structural Analysis: Crystals suitable for X-ray diffraction measurements were mounted on glass fibers. The diffraction data were collected with a Rigaku Mercury diffractometer using graphite-monochromated Mo-K_α radiation at –100 °C with the oscillation technique. Crystal data and experimental details are listed in Table 2. All structures were solved by a combination of direct methods and Fourier techniques. Non-hydrogen atoms were anisotropically refined by full-matrix least-squares calculations. Hydrogen atoms were included but not refined. Refinements were continued until all shifts were smaller than one-tenth of the standard deviations of the parameters involved. Atomic scattering factors and anomalous dispersion terms were taken from the International Tables for X-ray Crystallography.[35] All calculations were carried out with a Japan SGI workstation computer with the teXsan crystallographic software package.[36] CCDC-606977, CCDC-252730, CCDC-606976, and CCDC-281586 contain the supplementary crystallographic data for this paper. These data can be obtained free of charge from The Cambridge Crystallographic Data Centre via www.ccdc.cam.ac.uk/data_request/cif.

Other Physical Measurements

Elemental analysis was performed with a Perkin–Elmer 2400II CHNS/O full-automatic analyzer. All mass spectra were acquired with a LCT mass spectrometer equipped with an ionspray interface (Micromass Limited, Manchester, UK). Instrument settings, data acquisition, and data processing were controlled by a computer with Windows NT operating system. Samples were introduced with a single syringe pump (KD scientific Inc., USA) fitted with Hamilton syringes (Hamilton Co, Reno, NE). The samples for all spectral measurements were prepared in MeCN or MeOH. ^1H NMR spectra were recorded with a Varian Gemini-300 FT-NMR instrument. Electronic absorption spectra were measured with a JASCO V-550 or V-570 spectrophotometer in the wavelength range of 900 – 250 nm. A match paired quartz cell was used with a 10 mm length. Infrared spectral measurements were carried out with a JASCO FT/IR 410 spectrophotometer. Solid samples were prepared with a pressure greater than 5 tons in KBr powder. Spectra in solution were measured with the use of a double-piled CaF_2 or KBr cell with 0.1 mm thick walls for the C=O and S=O stretching frequencies of the sulfinates. Differential spectra between the sample and the corresponding solvent were used to verify the spectral features. Electrochemical measurements were performed with a BAS BIOANALYTICAL Systems model CV-50W or with a ALS/CH Instruments Electrochemical Analyzer Model 600A. Pt electrodes were adopted as the working- and counter-electrode and an Ag/Ag^+ electrode was used as a reference. Cyclic voltammograms were collected in a glove box under an Ar atmosphere. The potential values were revised on the Fc/Fc^+ standard.

Determination of Equilibrium Constants

Equilibrium constants were spectrophotometrically determined by means of spectral changes of **1** upon the addition of a suitable

Table 2. Crystallographic data and experimental details for Na[Co(**L:N_2S_2**)] (**1**-Na), PPh_4[Co(**L:N_2S_2**)] (**1**-PPh_4), PPh_4[Co(**L:N_2S_2**)(*t*BuNC)$_2$] (**2**) and PPh_4[Co{**L:$N_2(SO_2)_2$**}(*t*BuNC)$_2$] (**3**).

	1-Na	**1**-PPh_4	**2**	**3**
Empirical formula	$C_{11}H_{24}CoN_2O_5S_2Na$	$C_{35}H_{40}CoO_3N_2PS_2$	$C_{22.5}H_{28}Co_{0.5}ON_2P_{0.5}S$	$C_{47}H_{62}CoO_7N_4PS_2$
Formula mass	410.36	690.74	419.49	949.06
Crystal system	triclinic	monoclinic	tetragonal	monoclinic
Space group	$P\bar{1}$ (No. 2)	$P2_1/n$ (No. 14)	$P\bar{4}$ (No. 81)	$P2_1/a$ (No. 14)
a [Å]	9.949(3)	11.658(1)	16.7400(7)	10.4277(4)
b [Å]	9.958(3)	14.085(1)		33.484(1)
c [Å]	10.156(3)	20.977(2)	7.8718(5)	14.1350(5)
α [°]	69.48(2)			
β [°]	69.54(2)	100.159(4)		95.288
γ [°]	74.05(2)			
V [A^3]	869.5(5)	3390.3(5)	2205.9(2)	4914.4(3)
Z	2	4	4	4
$D_{calcd.}$ [$g\,cm^{-3}$]	1.567	1.353	1.263	1.283
F(000)	428.00	1448.00	888.00	2008.00
μ [cm^{-1}]	12.73	7.14	5.60	5.18
λ [Å]	0.71070	0.71070	0.71070	0.17070
T [K]	173	173	173	173
No. of refls. measured	6948	27401	17735	37445
No. of refls. used [$I > 2\sigma(I_0)$]	2892	5649	4584	8175
R_1[a]/R_w[b]	0.041/0.117	0.049/0.102	0.040/0.110	0.051/0.13
GOF	1.05	1.08	1.12	1.11

amount of *t*BuNC. The concentration of complex **1** was kept constant at $5.00 \cdot 10^{-5}$ mol dm^{-3}.

Supporting Information (see footnote on the first page of this article):Crystal packing of **1**-Na with hydrogen bonding interactions (Figure S1), crystal packing of **1**-PPh_4 (Figure S2), representative UV/Vis spectral change of **1**-PPh_4 due to the addition of monodentate ligand (Figure S3), ^{1}H NMR spectra of **1**-PPh_4 and **2** (Figure S4), UV/Vis spectra of **2** (Figure S5), plots of N≡C stretching vibration values for **3** versus ANs (Figure S6), tables of equilibrium constants, C=O stretching vibration values for **1** and **3**, S=O stretching vibration values for **3**, N≡C stretching vibration values for **3**, electrochemical parameters for **1** (Tables S1–S6) as PDF files.

Acknowledgments

This work was supported partly by a Grant-in-Aid for Scientific Research from the Ministry of Education, Science, Sports, and Culture of Japan (H.M. and Y. F.) and supported in part by a grant from the NITECH 21st Century COE Program, to which our thanks are due. We also thank to Prof. Masafumi Odaka, Tokyo University of Agriculture and Technology, who kindly provided useful comments about our results.

[1] T. Nagasawa, H. Yamada, *Trends Biotechnol.* **1989**, *7*, 153–158.
[2] M. Kobayashi, S. Shimizu, *Nature Biotechnol.* **1998**, *16*, 733–736.
[3] H. Yamada, M. Kobayashi, *Biosci. Biotechnol. Biochem.* **1996**, *60*, 1391–1400.
[4] M. Kobayashi, T. Nagasawa, H. Yamada, *Trends Biotechnol.* **1992**, *10*, 402–408.
[5] T. Nagasawa, K. Ryuno, H. Yamada, *Experientia* **1989**, *45*, 1066–1070.
[6] B. A. Brennan, G. Alms, M. J. Nelson, L. T. Durney, R. C. Scarrow, *J. Am. Chem. Soc.* **1996**, *118*, 9194–9195.
[7] M. J. Nelson, H. Jin, I. M. Turner Jr, G. Grove, R. C. Scarrow, B. A. Brennan, L. Que Jr, *J. Am. Chem. Soc.* **1991**, *113*, 7072–7073.
[8] M. Kobayashi, M. Nishiyama, T. Nagasawa, S. Horinouchi, T. Beppu, H. Yamada, *Biochim. Biophys. Acta* **1991**, *1129*, 23–33.
[9] W. Haung, J. Jia, J. Cummings, M. Nelson, G. Schneider, Y. Lindqvist, *Structure* **1997**, *5*, 691–699.
[10] S. Nagashima, M. Nakasako, N. Domae, M. Tsujimura, K. Takio, M. Odaka, N. Kamiya, I. Endo, *Nat. Struct. Biol.* **1998**, *5*, 347–351.
[11] A. Miyanaga, S. Fushinobu, K. Ito, T. Wakagi, *Biochem. Biophys. Res. Commun.* **2001**, *288*, 1169–1174.
[12] S. Hourai, M. Miki, Y. Takashima, S. Mitsuda, K. Yanagi, *Biochem. Biophys. Res. Commun* **2003**, *312*, 340–345.
[13] T. Murakami, M. Nojiri, H. Nakayama, M. Odaka, M. Yohda, N. Dohmae, K. Takio, T. Nagamune, I. Endo, *Protein Science* **2000**, *9*, 1024–1030.
[14] a) J. J. Ellison, A. Nienstedt, S. C. Shoner, A. Basrnhart, J. A. Cowen, J. A. Kovacs, *J. Am. Chem. Soc.* **1998**, *120*, 5691–5700; b) J. Shearer, I. Y. Kung, S. Lovell, W. Kaminsky, J. A. Kovacs, *J. Am. Chem. Soc.* **2001**, *123*, 463–468; c) A. Dey, M. Chow, K. Taniguchi, P. Lugo-Mas, S. Davin, M. Maeda, J. A. Kovacs, M. Odaka, K. O. Hodgson, B. Hedman, E. I. Solomon, *J. Am. Chem. Soc.* **2006**, *128*, 533–541.
[15] a) J. C. Noveron, M. M. Olmstead, P. K. Mascharak, *J. Am. Chem. Soc.* **1999**, *121*, 3553–3554; b) L. A. Tyler, J. C. Noveron, M. M. Olmstead, P. K. Mascharak, *Inorg. Chem.* **2003**, *42*, 5751–5761; c) J. C. Noveron, M. M. Olmstead, P. K. Mascharak, *J. Am. Chem. Soc.* **2001**, *123*, 3247–3259.
[16] T. Ozawa, T. Ikeda, T. Yano, H. Arii, S. Yamaguchi, Y. Funahashi, K. Jitsukawa, H. Masuda, *Chem. Lett.* **2005**, *34*, 18–19.
[17] a) C. A. Grapperhaus, A. K. Patra, M. S. Mashuta, *Inorg. Chem.* **2002**, *41*, 1039–1041; b) C. A. Grapperhaus, M. Li, A. K. Patra, S. Poturovic, P. K. Kozlowski, M. Z. Zgierski, M. S. Mashuta, *Inorg. Chem.* **2003**, *42*, 4382–4388.
[18] a) M. Rat, R. A. de Sousa, J. Vaissermann, P. Leduc, D. Mansuy, I. Artaud, *J. Inorg. Biochem.* **2001**, *84*, 207–213; b) E. Galardon, M. Giorgi, I. Artaud, *Chem. Commun.* **2004**, 286–287; c) S. Chatel, M. Rat, S. Dijiols, P. Leduc, J. P. Tuchagues, D. Mansuy, I. Artaud, *J. Inorg. Biochem.* **2000**, *80*, 239–246; d) E. Bourles, R. A. de Sousa, E. Galardon, M. Giorgi, I. Artaud, *Angew. Chem. Int. Ed.* **2005**, *44*, 3526–3528.
[19] a) L. Heinrich, Y. Li, J. Vassermann, J.-C. Chottard, *Eur. J. Inorg. Chem.* **2001**, 1407–1409; b) L. Heinrich, A. Mary-Verla, Y. Li, J. Vassermann, J.-C. Chottard, *Eur. J. Inorg. Chem.* **2001**, 2203–2206; c) L. Heinrich, Y. Li, K. Provost, A. Michalowicz, J. Vassermann, J.-C. Chottard, *Inorg. Chim. Acta* **2001**, *318*, 117–126; d) L. Heinrich, A. Mary-Verla, J. Vassermann, J.-C. Chottard, Y. Li, *Inorg. Chim. Acta* **2004**, *357*, 117–126; e) L. Heinrich, Y. Li, J. Vassermann, G. Chottard, J.-C. Chottard, *Angew. Chem. Int. Ed.* **1999**, *38*, 6162–6165.
[20] M. Rat, R. A. de Sousa, A. Tomas, Y. Frapart, J.-P. Tuchagues, I. Artaud, *Eur. J. Inorg. Chem.* **2003**, *4*, 759–765.
[21] S. R. Piersma, M. Nojiri, M. Tsujimura, T. Noguchi, M. Odaka, M. Yohda, I. Endo, *J. Inorg. Biochem.* **2000**, *80*, 283–288.
[22] A. Miyanaga, S. Fushinobu, K. Ito, H. Shoun, T. Wakagi, *Eur. J. Biochem.* **2004**, *271*, 429–438.
[23] K. Taniguchi, M. Tsujimura, M. Odaka, T. Hirose, I. Endo, M. Maeda, *1st Joint Symposium on Biofunctional Chemistry and Biotechnology* **2003**, Oct. 12–13, Kumamoto University, Japan.
[24] H. Suzuki, M. Nojiri, N. Kamiya, T. Noguchi, *J. Biochem.* **2004**, *136*, 115–121.
[25] A. Taha, M. M. Mahmoud, *New J. Chem.* **2002**, *26*, 953–957.
[26] Q. Liu, D. Fang, J. Zheng, *Spectrochim. Acta, Part A* **2004**, *60*, 1453–1458.
[27] Q. Liu, X. Xu, W. Sang, *Spectrochim. Acta, Part A* **2003**, *59*, 471–475.
[28] H. Muta, K. Ishida, E. Tamaki, M. Satoh, *Polymer* **2003**, *43*, 103–110.
[29] R. W. Taft, N. J. Pienta, M. J. Kamlet, E. M. Arnett, *J. Org. Chem.* **1981**, *46*, 661–667.
[30] V. Gutmann, *Electrochim. Acta* **1976**, *21*, 661–670.
[31] S. Chatel, A.-S. Chauvin, J.-P. Tuchagues, P. Leduc, E. Bill, J.-C. Chotard, D. Mansuy, I. Artaud, *Inorg. Chim. Acta* **2002**, *336*, 19–28.
[32] T. J. Collins, *Acc. Chem. Res.* **1994**, *27*, 279–285.
[33] L. A. Tyler, M. M. Olmstead, P. K. Mascharak, *Inorg. Chem* **2001**, *40*, 5408–5414.
[34] G. Garminati, P. Galimrerti, M. Melandri, *Boll. Chim. Farm.* **1963**, *102*, 522–540.
[35] *International Tables for X-ray Crystallography* (Eds.: J. A. Ibers, W. C. Hamilton), Kynoch Press, Birmingham, U. K., **1974**, vol. IV.
[36] *Texsan, Crystal Structure Analysis Package*, Molecular Structure Corporation (1985), **1992**.

Received: May 15, 2006
Published Online: August 3, 2006

